Available online at www.sciencedirect.com
SCIENCE DIRECT®
Journal of volcanology and geothermal research
ELSEVIER
Journal of Volcanology and Geothermal Research 3001 (2004) 1–15
www.elsevier.com/locate/jvolgeores

Viscoelastic behaviour of basaltic lavas

M.R. James [a,b,*], N. Bagdassarov [a], K. Müller [a], H. Pinkerton [b]

[a] *Institut für Meteorologie und Geophysik, J.W. Goethe Universität Frankfurt, Frankfurt am Main, Germany*
[b] *Department of Environmental Science, I.E.N.S., Lancaster University, Lancaster LA1 4YQ, UK*

Received 3 December 2001; accepted 15 July 2003

Abstract

The rheological properties of basaltic lavas from Etna, Hawai′i and Vesuvius have been investigated at temperatures between ~500 and 1150°C using a small-strain oscillatory shear. The viscoelastic response of the lavas to small, forced, sinusoidal torques ($<10^{-3}$ N m) at frequencies between 0.002 and 20 Hz was measured. A purely viscous regime was only approached during experiments with Hawai′i samples. These experiments indicated that at temperatures between ~1070 and 1130°C, strain rate-independent viscosities ($>10^9$ Pa s) could be measured at strain rates less than ~10^{-2}–10^{-1} s^{-1}. At 800°C, temporal variations in complex shear modulus and internal friction suggest that, over durations of up to 120 h, structural adjustments were occurring within some of the samples. This time-varying behaviour of lava samples may be attributed to the slow closing (healing) of microcracks and small pore spaces, resulting in the apparent stiffening of lava samples under annealing. Thus, those parts of lava flows that undergo slow cooling will have more elastic properties. Regions that cool faster possess smaller shear moduli and higher internal friction due to thermal microcracking and less cohesion between crystals and the bulk glassy matrix.

Keywords: basalt lava; Etna; Vesuvius; Hawai′i; shear modulus; shear viscosity; oscillatory rheology

1. Introduction

The rheological properties of basaltic lava are critical parameters in determining the advance rates, morphology and final dimensions of basaltic flows. Rheology is controlled by a number of factors, the most important of which are composition, temperature, crystallinity and bubble content. The effects of these factors on the viscosity of lavas between eruption and solidification have been analysed by previous workers (Shaw et al., 1968; Sparks and Pinkerton, 1978; Marsh, 1981; Ryerson et al., 1988; Pinkerton and Stevenson, 1992; Pinkerton and Norton, 1995; Richet et al., 1996; Dingwell et al., 1998). At temperatures below their eruption temperature, lavas display viscoelastic behaviour and, at temperatures below the glass transition temperature, T_g, of their glass matrix, they are anelastic (Sakuma, 1953; Bagdassarov, 2000). Field measurements carried out at high stresses (~10^3 Pa) and typical eruption temperatures indicate that basaltic lavas have a rather moderate viscosity ($>10^2$ Pa s) and an appreciable static yield strength (~10^2–10^3 Pa) (Shaw et

* Corresponding author. Tel.: +44-1524-593574; Fax: +44-1524-593985.
E-mail addresses: m.james@lancs.ac.uk (M.R. James), nickbagd@geophysik.uni-frankfurt.de (N. Bagdassarov), h.pinkerton@lancs.ac.uk (H. Pinkerton).

0377-0273/03/$ – see front matter © 2003 Published by Elsevier B.V.
doi:10.1016/S0377-0273(03)00340-8

al., 1968; Pinkerton and Sparks, 1978; Pinkerton and Norton, 1995; Norton and Pinkerton, 1997).

The stiffness of solidifying lava, the temperature range over which solidification and the anelastic transformation occur and the kinetics of fracturing and fracture healing processes are important parameters for lava flow modelling. Quantification of these processes may be important, for example, in the prediction of lava flow carapace generation or break-up. Here, we present the results of viscoelastic measurements carried out on samples of basalt lava flows taken from Etna, Hawai'i and Vesuvius at temperatures in the range ~500–1150°C. These reveal the importance of cooling rate of lava flows on the strength of lavas.

Experiments designed to characterise the high-temperature anelastic and viscoelastic behaviours of glassy, crystalline and partially molten rocks are based on measurements of elastic modulus (G^*) and internal friction (Q^{-1}). Traditionally, these measurements are performed using an inverted torsional pendulum (e.g. Day and Rindone, 1961; Gueguen et al., 1981; Weiner et al., 1987; Versteeg and Kohlstedt, 1994) or by forced torsional oscillation (Berckhemer et al., 1982; Jackson and Paterson, 1987; Bagdassarov and Dingwell, 1993; Gribb and Cooper, 1998). The forced torsional oscillation method used in this work has previously been used to study the behaviour of both rocks (Berckhemer et al., 1982; Jackson and Paterson, 1987; Gribb and Cooper, 1998; Bagdassarov and Dorfman, 1998) and glasses (Bagdassarov and Dingwell, 1993; Bagdassarov et al., 1993, 1994). This technique allows the magnitude of the complex shear modulus and angle of internal friction to be measured over a range of temperatures and frequencies.

2. Apparatus

The experimental method consists of exerting small-strain oscillatory torsion deformation on cylindrical samples. The equipment (described in detail previously (Berckhemer et al., 1982; Kampfmann and Berckhemer, 1985; Bagdassarov and Dingwell, 1993)) exerts a small sinusoidal torque (of amplitude $\sim 10^{-3}$ N m) to the end of a cylindrical sample (8 mm in diameter, ~20–30 mm in length). A simple schematic of the device is shown in Fig. 1a. The sinusoidal torque applied to the sample is generated using a pair of electromagnets (two microphone-type coils) connected to a synthesiser via a power amplifier. The sample is fixed between two aligned alumina rods, onto which two sets of light aluminium wings are also attached. The angular deformation across the sample is measured by pairs of capacitive pick-ups which respond to the movement of pure iron plates located at the ends of the aluminium wings. The capacitive signal is detected and amplified using a 5-kHz frequency bridge which is sampled using a PC. Calibration of the equipment has been described previously (Bagdassarov, 2000), with shear modulus measurements being accurate to 3–5% (due to thermal drift of the calibration at high temperatures).

Although the mechanical design of the equipment has not changed from that used during previous work, the data acquisition hardware and processing software have been significantly improved. For each measurement, data are collected over two periods of the torsional oscillation (Fig. 1b). Data are sampled at up to 10 kHz, allowing 1000 samples per channel to be acquired at the highest frequency used during experiments (20 Hz). At torsional oscillation frequencies of 2 Hz or lower the number of samples per channel is limited to 10 000. Sinusoids are automatically fitted to the collected data using a Levenberg–Marquardt algorithm, and the shear modulus and phase difference between the applied torque and the angular displacement across the sample are calculated from the phase and amplitude parameters of the fitted curves.

Experiments were carried out over the frequency range 0.002–20 Hz (at approximately 0.3 log intervals) and at temperatures between ~500 and 1150°C. At high temperatures, low-frequency measurements were prevented by the onset of non-linear sample response. This was revealed by Fourier analysis of the data indicating the presence of harmonics of the torsional driving frequency. Automation of sampling and processing allows repeated measurements and at high

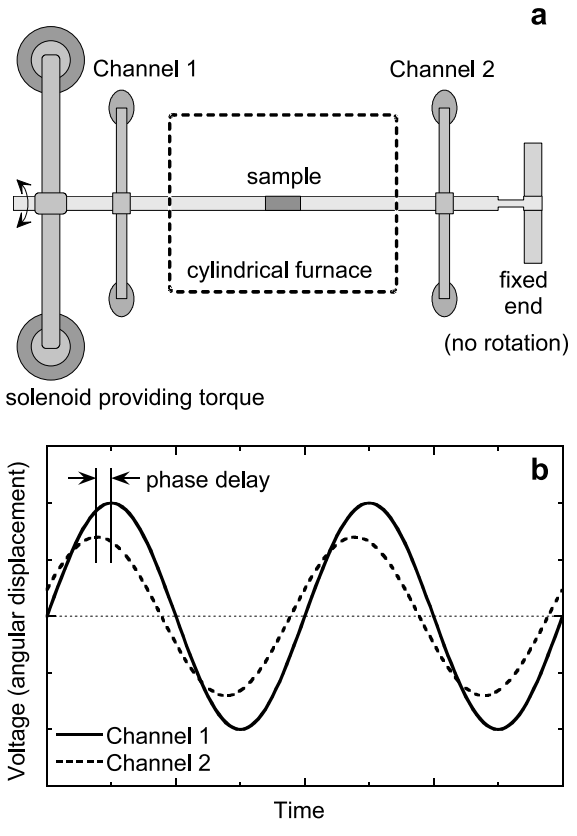

Fig. 1. (a) Schematic of the torsion oscillation apparatus (redrawn from Berckhemer et al., 1982). Capacitive pickups detect the motion of the iron plates at the ends of the aluminium wings, providing two data channels that can be calibrated to provide angular deflection and the applied torque. (b) An example of two periods of data collected in order to measure internal friction (from the phase shift) and magnitude of the complex shear modulus (from the relative amplitudes of the curves). Further details are given in Bagdassarov (2000).

frequencies an average of 20 measurements was used for most temperature–frequency points. At low frequencies, individual measurements take up to 17 min, so fewer experiments were averaged.

During experiments the furnace was purged with a flow of Ar gas (5 cm^3 s^{-1}). Inspection of the samples after experiments showed that oxidation (as indicated by growth of Fe–(Ti)-oxides) had taken place only on the surfaces of the samples. Temperatures were recorded using Pt–PtRd (S-type) or Ni–NiCr (K-type) thermocouples. Direct measurements of the temperature field inside the furnace indicated that temperatures were reduced by up to 15°C at distances of 10 mm from the hottest point. Although this spatial sensitivity implies that recorded values were only accurate to ~15°C as indicators of the sample temperature, relative temperature changes within any one experiment are much better constrained (±3°C at 1000°C).

The data collected at each temperature–frequency point allowed calculation of the magnitude of the complex shear modulus $G^*(\omega, T)$, and the phase shift $\varphi(\omega,T)$ between the applied torque and the resultant angular strain of the sample, where ω is the angular velocity (equal to 2π multiplied by the applied frequency). From these results, the real, G', and the imaginary, G'', parts of the complex shear modulus, the internal friction, Q^{-1}, and the complex shear viscosity, η, can be calculated from:

$$G^* = G' + iG'' = G^*\cos(\varphi) + iG^*\sin(\varphi) \quad (1)$$

$$Q^{-1} = \tan(\varphi) = \frac{G''}{G'} \quad (2)$$

$$\eta = \eta' - i\eta'' = \frac{G''}{\omega} + i\frac{G'}{\omega} \quad (3)$$

(e.g. Nowick and Berry, 1972). The zero-rate shear viscosity (macroscopic viscosity), η_0, may be obtained from the frequency dependence of G'' by:

$$\eta_0 = \lim_{\omega\to 0}\frac{G''(\omega)}{\omega} \quad (4)$$

(Marin, 1998).

2.1. Sample bonding

During experiments it is essential that each end of the sample is securely bonded to the alumina rods. In order to do this efficiently, small conical grips (angle ~1°, length 4 mm) were machined at both flat ends of the sample with a diamond tool. Complementary mating grips were produced in the alumina rods and samples were cemented between the rods with a high-temperature cement (Polytec®). The assembly was placed in the torsion apparatus and the sample was then sintered to the rods for 2 h at 150°C and then for 24 h at

500°C, under an axial load of ~8 N (e.g. Berckhemer et al., 1982). Measurements carried out using a dummy sample of Al_2O_3 have demonstrated that the effect of the cement on phase delay measurements was less than 10^{-3} rad (Bagdassarov and Dorfman, 1998).

2.2. Size and shape factors

When temperatures increased during experiments, thermal expansion of the sample and the alumina ceramic rods was accommodated by a spring located at one end of the apparatus. At temperatures sufficiently high for the sample to deform, some of the accumulated stress dissipates by flow shortening of the sample. Changes in sample length were calculated from micrometer readings taking at the spring (to a precision of ~0.02 mm) and the correspondingly changed sample diameter (calculated by assuming conservation of sample volume) were then used to calculate the material properties. However, samples recovered after experiments have shown that flow deformation was not continuously distributed through the samples but was concentrated in the centre, producing distorted, barrel-shaped, cylinders. This is a consequence of temperature gradients across the sample and due to it being supported at both ends. Thus, despite efforts to account for changes in the sample shape, the deviation from a cylindrical form introduced errors (<2%) in the assumed diameter of the sample, once sample shortening has started.

2.3. Sample description

The experiments were carried out on samples of basaltic lavas collected from three different volcanoes, Etna, Hawai′i and Vesuvius.

2.3.1. Etna

Two samples from Etna were collected from lava erupted in 1992 which had ponded after overflowing from a skylight in the Valle del Bove. One of these samples was from the top surface and one was taken from the base (~10 cm down from the surface) and thus represent samples with different cooling regimes. Digital images of polished sections were obtained through an optical microscope and computer-analysed, omitting corrections for 3D effects. The surface sample has smaller vesicles (~0.2–0.5 mm, 15–20 vol%) and smaller crystal content (~20–30 vol%) than the basal sample (~20 vol% of 1–2 mm vesicles and ~30 vol% phenocrysts). Images of polished thin sections are shown in Fig. 2. A further sample was collected from near the southeast cone in 1999. This sample was taken from the least vesicular area found in a recently emplaced flow near hornito H3 (Calvari and Pinkerton, 2002) at the top of the active flow field.

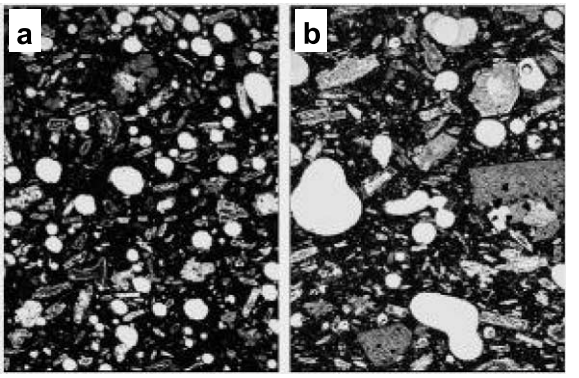

Fig. 2. (a) Thin section of the crustal sample from Etna, 1992. The lava contains ~15–20 vol% of vesicles (mean diameter between ~0.2 and 0.5 mm) and ~20–25 vol% of plagioclase, olivine and magnetite phenocrysts. (b) Thin section of the 1992 Etna sample that was collected from the base of an overflow. This sample contains ~20 vol% of vesicles with a mean diameter of 1–2 mm and about 30 vol% of crystal (from analysis of polished thin sections without corrections for 3D effects).

2.3.2. Hawai′i

The Hawaiian basalt was sampled in the east rift eruption zone of Kilauea, Hawai′i, from a lava flow from a pahoehoe toe in September, 1984 (eruption temperature ~1147°C). This pahoehoe lava flow corresponds to episode 25 of the eruption Pu′u ′O′o of Kilauea Volcano. Its bulk chemical composition has been presented elsewhere (Garcia et al., 1992). The chemical composition of the groundmass glass obtained by microprobe analysis differs from the bulk rock composition in SiO_2 (52.3 wt%) and CaO (9.2%) content (Bagdassarov, 2000). The vesicularity es-

timated from 2D image analysis varies from 46.8 to 57.6 vol%, or ~50 vol% when calculated on the 'dry' density rock basis. The sample has about ~10 vol% of olivine quenched from magma during sampling and a few percent of other phenocrysts.

2.3.3. *Vesuvius*

The Vesuvius samples were collected from the 1834 flow at Cava Ranieri in the national protected area of Terzigno approximately 6.3 km ESE of the central cone of Vesuvius by the group from University College of London. Chemical analysis of the samples is given in Belkin et al. (1993). The same sample was also used by Rocchi et al. (2002) in experiments to determine Young's modulus and tensile strength.

3. Results

The shear modulus and internal friction results for the samples are given in Figs. 3–6. The 1992 Etna samples (Fig. 3) show marked differences in shear modulus and internal friction between the rapidly cooled crustal sample and the more slowly cooled basal sample. As a result of its smaller volume fraction of vesicles, the crustal sample has a shear modulus ~1.5–2 times greater than that of the basal sample at high temperatures (>1050°C), increasing to ~six times at low temperatures (~500°C). The internal friction of the crustal sample shows a relatively low dependence on frequency at high temperatures (>800°C). At temperatures between ~600 and 800°C (Fig. 3c) a small, wide peak in internal friction suggests a complicated behaviour at temperatures corresponding to that of the glass transition for basaltic glass (Ryan and Sammis, 1981). For Pu′u ′O′o pahoehoe lavas, the glass transition and melting temperatures are 655 and 1149°C, respectively (Burkhard, 2001). In contrast, at temperatures below 1000°C, the internal friction of the basal sample (Fig. 3d) is a strong power law of frequency,

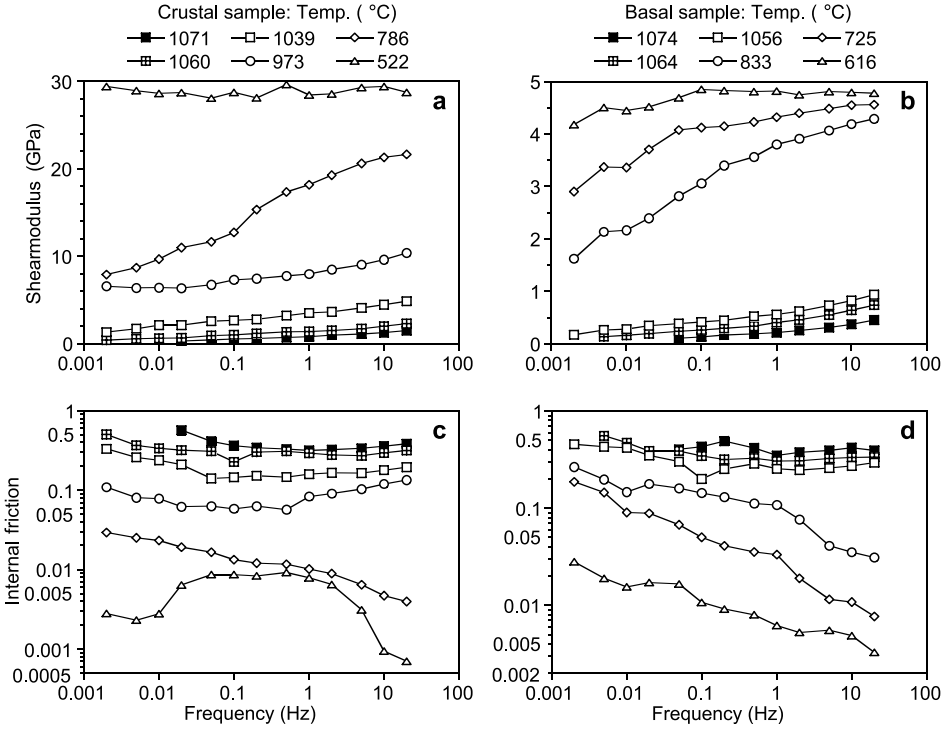

Fig. 3. Shear modulus (a,b) and internal friction (c,d) results from the 1992 Etna lavas. The crustal sample (a,c) shows a higher shear modulus than the basal sample, and neither sample has an internal friction approaching 1 over the conditions investigated.

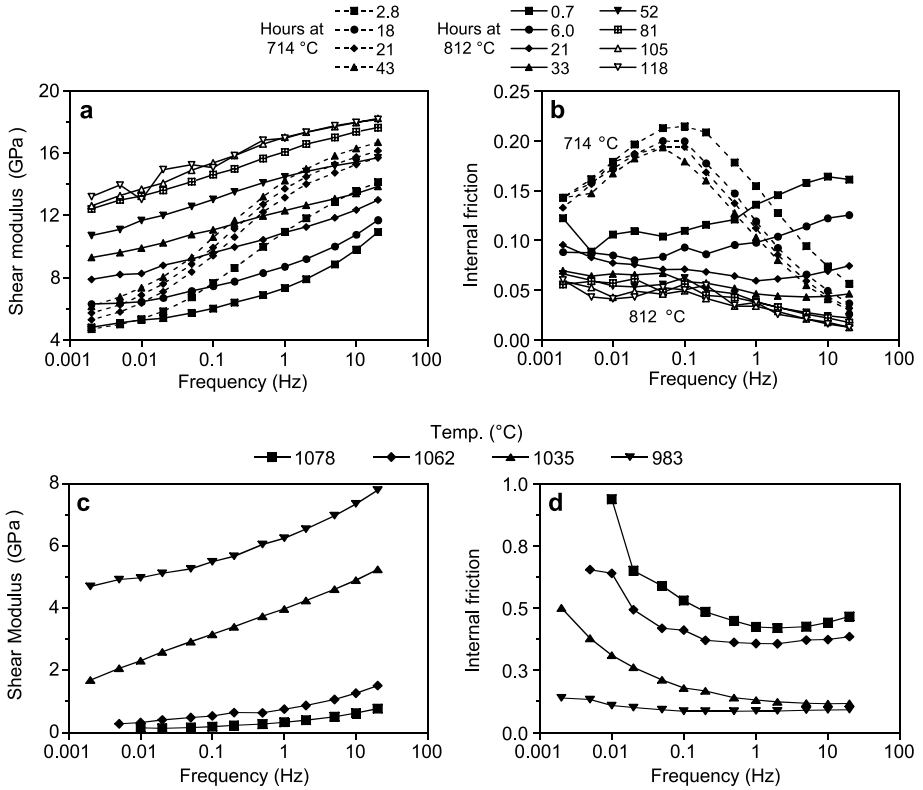

Fig. 4. In panels and b, temporal variations in shear modulus and internal friction are given for the 1999 Etna sample. After annealing for 118 h at 800°C the sample had attained a greater shear modulus than it originally possessed at 700°C. The increasing shear modulus and decreasing internal friction with time indicate the sample was becoming increasingly elastic and less viscous. The shear modulus and internal friction results collected after annealing are given in panels c and d.

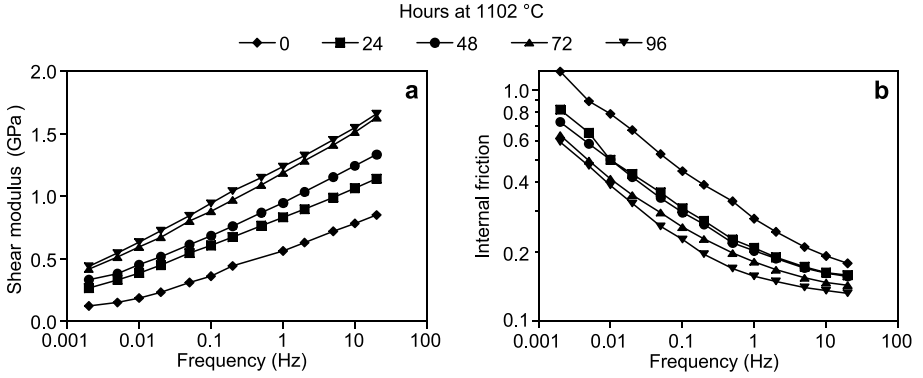

Fig. 5. Time-dependent shear modulus (a) and internal friction (b) during annealing experiments on the Hawai'i sample. Numbers in the legend indicate annealing time in hours.

$Q^{-1} \propto \omega^{-0.35}$. The response of a purely elastic material would be independent of frequency, and this frequency dependence indicates a partially viscous response even at ~600°C.

Similar experiments carried out on cores cut from the 1999 Etna sample not only reproduced the internal friction peak at low temperatures (~700°C) but demonstrated considerable temporal variations in the results (Fig. 4). Over periods of up to ~120 h, the measured shear modulus increased and internal friction decreased. After annealing, the 1999 samples produced similar shear modulus and internal friction results (Fig. 4c,d) to those of the 1992 Etna crustal material. At temperatures >1100°C, Etna samples demonstrated an increase of fluidity of several orders of magnitude and it was not possible to maintain them in the torsion apparatus.

The experiments carried out on the Hawai′i sample were extended to higher temperatures because of the higher temperature of the sample's softening point. Similar temporal variations to those observed with the Etna lavas were found and are shown in Fig. 5 at a temperature of 1102°C. The results are broadly similar to those of the Etna samples, with shear moduli of ~18 GPa decreasing to ~0.2 GPa as sample fluidity starts to rapidly increase.

The results from the experiments carried out on the Vesuvius sample are given in Fig. 6. During sample annealing the shear modulus increased but to a lesser extent than in Etna samples. An increase in tensile strength and Young's modulus after annealing was also reported during bending experiments (Rocchi et al., 2002). At the highest temperature attained during experiments (1132°C) the shear modulus was less than 0.5 GPa and practically frequency-independent. With a further increase of temperature the sample became too fluid for it to be held within the torsion apparatus.

4. Discussion

Measurements of the complex shear modulus (G^*) and internal friction (Q^{-1}) of lava samples from Etna, Vesuvius and Hawai′i show that they possess an appreciable shear modulus (>0.5 GPa) and an internal friction generally less than 1, at temperatures where field measurements indicate viscosities of ~10^3 Pa s. For comparison, polycrstalline rocks at room temperature have typical values of unrelaxed shear modulus, G_∞, of about 50 GPa (Jackson, 1993) and 25 GPa is representative for silicate glasses (Bagdassarov et al., 1993). Between room and high temperatures prior to the onset of melting, values of Q^{-1} vary between ~10^{-3} and 10^{-1} (Manghnani et al., 1981; Weiner et al., 1987; Jackson, 1993; Bagdassarov, 2000).

Natural silicate melts and glasses show a linear viscoelastic behaviour in the glass transition temperature range (e.g. Bagdassarov and Dingwell, 1993; Bagdassarov et al., 1993). With increasing temperature and decreasing strain rate, one ex-

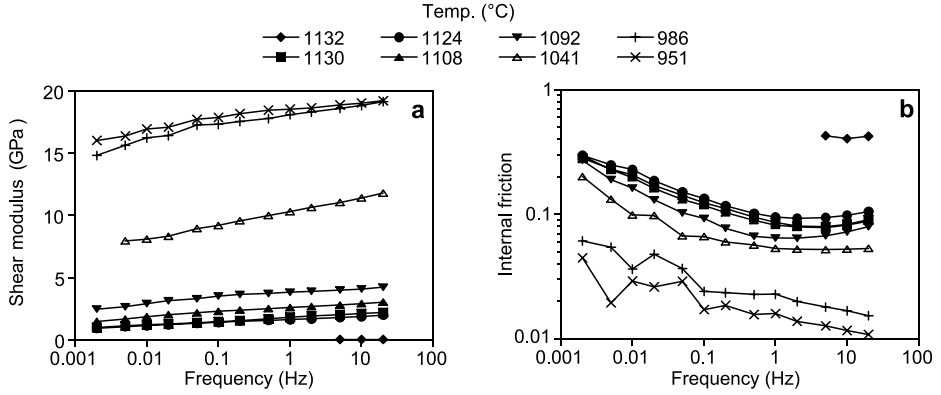

Fig. 6. Shear modulus (a) and internal friction (b) results from the Vesuvius lava.

pects progressively decreasing shear modulus and increasing internal friction. However, the viscoelastic behaviour of lavas is often controlled by the presence of deformable (vesicles) and non-deformable (crystals) heterogeneities. Viscosity increases with increasing crystal content but decreases with increasing vesicle content (Bagdassarov and Dingwell, 1992) and the presence of these macroscale obstacles extends the shear stress relaxation spectrum towards longer relaxation times. Shear modulus relaxation can be extended over several hundred °C above the T_g of a basaltic groundmass glass ($\sim$655°C) up to $\sim$1100–1150°C. Over the same range, the frequency dependence of shear modulus and internal friction becomes weaker, for example, in lavas $Q^{-1} \propto \omega^{-0.35}$, compared to $\omega^{-0.5}$ for silicate melts.

The shear modulus and internal friction of our lava samples varied significantly with annealing time with, at temperatures between $\sim$500 and 1000°C, some samples becoming increasingly stiff and elastic (Fig. 4). Similar temporal variations of elastic modulus and internal friction have been previously observed in thermally cycled quartzite, granite, dunite and sandstones (Johnson and Toksöz, 1980; Jackson, 1993; Lu and Jackson, 1998) and is thought to be due to the presence and healing of microcracks and pores. For example, rapid thermal cycling of granite and diabase samples from room temperature to $\sim$800°C results in order of magnitude increases in crack porosity and a factor of 2 increase in Q^{-1} due to the thermal production of cracks (Johnson and Toksöz, 1980). Jackson (1993) interpreted the observed increase in shear modulus and decrease in internal friction with the increasing annealing time to be a result of the reduction of porosity and increase of the grain boundary cohesion by a sintering process. Progressive decreases in Q^{-1} have been associated with a decrease of centres of stress concentration. Thus, we interpret our data, which indicate an increasingly elastic response with time, as demonstrating the effects of healing microcracks and thermally produced pore space (not vesicles) in the samples. It is likely that the microcracks were originally created due to thermal stresses during rapid cooling of the lava flows; however, we cannot exclude the possibility that they could have been produced during sample preparation or the subsequent heating. In thin

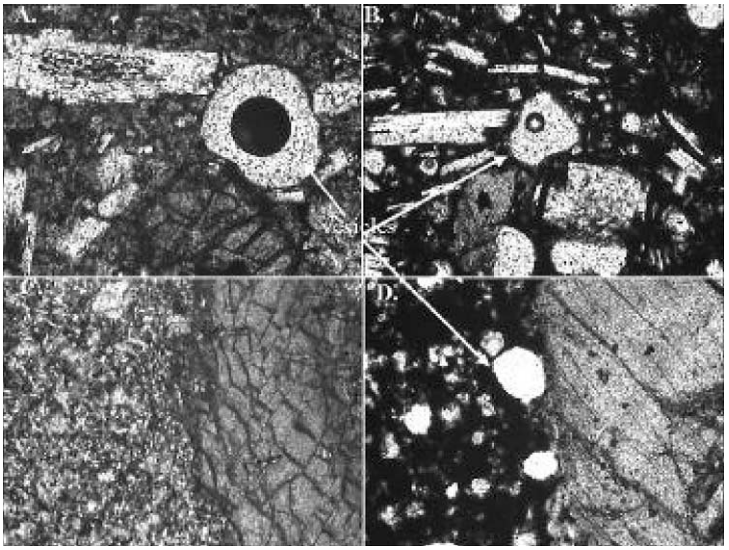

Fig. 7. Thin sections of Etna (A,B) and Vesuvius (C,D) lava samples (each image represents 1250×950 μm). Panels A and B give starting material and show microcracks between crystals and groundmass glass as well as in the interior of phenocrysts. Panel B shows the Etna sample after being annealed at 812°C for 118 h and panel D shows the Vesuvius sample after being annealed at 1102°C for 96 h. The reduction in the number of microcracks demonstrates that healing has occurred both within the groundmass and the phenocrysts.

sections, microcracks within crystals and between crystals and the groundmass can be observed to have undergone some healing after annealing (Fig. 7).

The production of microcracks suggests that rocks which have undergone slow cooling will possess higher shear moduli and have higher strengths than rocks which cooled more rapidly. Thus, before annealing, samples taken from the centre of a cooled flow would be expected to be more elastic than samples taken from the top of a flow. Under annealing at high temperature, the crack healing process consists of cracks pinching off and healing to a pore-like shape before subsequent decreasing of the pore diameter (Atkinson, 1984). During this period, the shear modulus may significantly increase and the internal friction decrease. The time dependence of changes in crack lengths can be described as an Arrhenius function of temperature and, as a first approximation, a linear dependence between shear modulus and a crack density parameter may be assumed (O'Connel and Budiansky, 1974). In Fig. 8a the results of annealing on the complex shear modulus of the 1999 Etna lava sample are presented as a function of time, t. By fitting these data with an exponential time dependence:

$$|G^*| = (G_\infty - G(0))\{1 - e^{-t/\tau}\} + G(0) \quad (5)$$

where G_∞ is the stable shear modulus at any temperature, $G(0)$ is the shear modulus at $t = 0$, the characteristic time, τ, of the crack healing process may be estimated. The results of the fitting are presented in Fig. 8b in the form of an Arrhenian dependence of τ, yielding an activation energy of 150 ± 20 kJ mol^{-1}. According to Atkinson (1984) this value should relate to the activation energy of the effective diffusion coefficient on grain boundaries of species participating in the pinching process at microcrack tips. For example, the activation energy of crack healing in dry quartz at $T < 600$°C is about 80–85 kJ mol^{-1} (Atkinson and Meredith, 1987), corresponding to the activation energy of water diffusion in quartz ($\sim$60 kJ mol^{-1}, Dersch et al. (1997) or $\sim$100 kJ mol^{-1}, Brady (1995)). At high temperatures, crystal lattice diffusion is the rate-controlling mechanism of grain boundary diffusion. Thus, the observed activation energy for the time dependence of shear modulus may be associated with an inter-diffusion of Ca, Mg and alkaline species between olivine, clinopyroxene and plagioclase crystals and basalt glass, with activation energies between 130 and 180 kJ mol^{-1} (Brady, 1995). Alternatively, our results are also consistent with a self-diffusion of Si and O, network formers in basaltic glass, with an activation energy of 170 kJ mol^{-1} (Lesher et al., 1996).

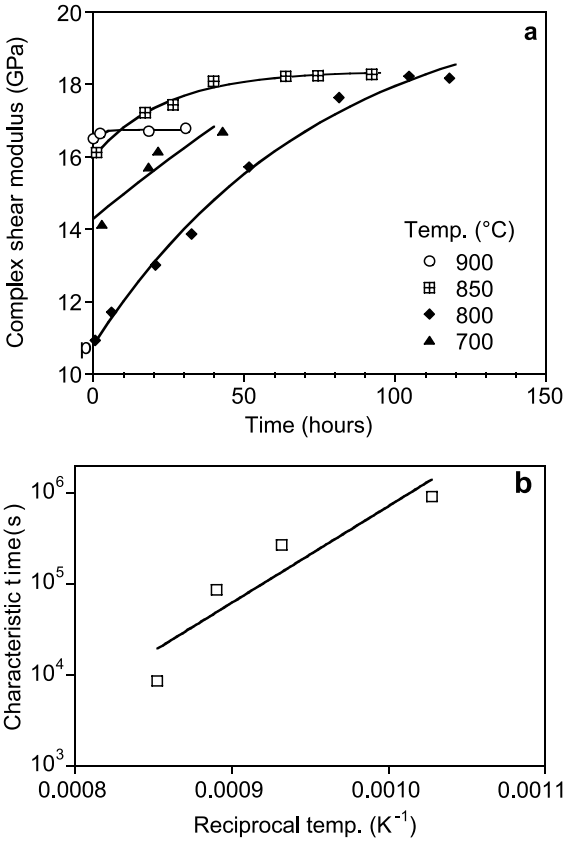

Fig. 8. (a) The complex shear modulus of 1999 Etna lava measured at 20 Hz and different temperatures. The temporal change at each temperature is modelled using a curve of characteristic time constant that is believed to represent the characteristic time for crack healing (see text). In panel b, these characteristic times are plotted against absolute reciprocal temperature. The straight line fit represents an Arrhenian dependence with an activation energy of 150 ± 20 kJ mol^{-1}.

Alternative mechanisms that could contribute to the increase of shear modulus during annealing of samples are redox and re-crystallisation pro-

cesses in the basalt groundmass glass. Progressive volatile loss could also be responsible for strengthening the samples; however, this cannot explain the power law frequency dependence of internal friction in the 1992 Etna samples at low temperatures. A contribution to shear modulus increase from sample oxidation would be due to the production of interface-controlled intergrowths of pyroxene dendrites and Fe–(Ti)-oxides between 850 and 940°C (Burkhard, 2001). However, the activation energy of this process is ~100 kJ mol^{-1}, which is less than that observed from the time variation curves of shear modulus. The oxidation kinetics of basaltic glass are determined primarily by the diffusion of divalent cations Ca^{2+} and Mg^{2+} to the surface of the sample, which is charge-compensated by the inward flux of electron holes (Cooper et al., 1996). The activation energy of this process at temperatures below T_g is 210 kJ mol^{-1}. The calculated maximum depth (~1 μm at 600°C and ~20 μm at 800°C) of surface oxidation by using the average divalent cation diffusion coefficient (Cooper et al., 1996) is small compared with the size of lava samples used in torsion experiments and is in agreement with observations made from thin sections of the samples. It should also be noted that these rates relate to initially non-oxidised basalt glass samples and the lava samples should be considered as slow-cooled, partially crystallised glasses, with long oxidation histories.

At $T > 920$°C, the bulk crystallisation of basaltic glass and growth of plagioclase crystals may also contribute to the increase of stiffness of annealed lava samples, but the timescales required are generally much longer than those of the observed changes in shear modulus. For example, a noticeable growth of plagioclase and Fe–Ti-oxides has been observed at 850–934°C after >200 h of annealing basalt glass (Burkhard, 2001) and this process is likely to have continued for an order of magnitude longer time. In contrast, shear modulus changes occurred much more rapidly in our experiments and generally ceased on a timescale of <100 h. Thus, neither redox nor re-crystallisation processes are believed to significantly contribute to the measured changes in the rheological properties of the samples.

Converting the shear modulus and internal friction data into viscosity (Eq. 3) shows that both the Vesuvius and Etna samples maintained a frequency-dependent real component of their viscosity (η') up to the highest temperatures attainable during the experiments (Fig. 9). Therefore, no 'Newtonian' viscosity can be given for these temperatures at low strain rates. In contrast, the Hawaiian sample demonstrated marked decreases in the frequency dependence of η' at high temperatures and low frequencies (Fig. 10a). The main difference between the low strain rate behaviour of, on the one side, Etna and Vesuvius basalts, and, on the other, that from Hawai'i, lies in the relative proportion of crystals and vesicles. The small strain rate and small stress viscosity, η_0, measured for the Hawaiian sample represent a creep-type mechanism underlying the Bingham yield stress which is expressed under conditions of slow, small-scale deformation, where the inter-

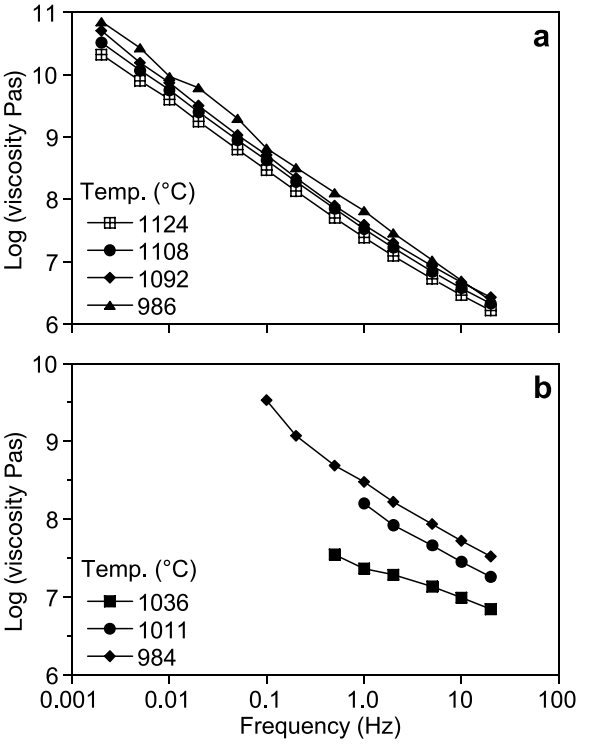

Fig. 9. Dynamic viscosity as given by $G''(\omega)/\omega$ (see Eq. 4) for the Vesuvius (a) and Etna (b) samples. At the highest temperatures and lowest frequencies used these samples maintained a frequency-dependent rheology.

nal structure of the lava sample remains intact. The presence of non-deformable crystals results in increases of this effective viscosity, but also increases the Bingham yield stress (Bagdassarov et al., 1994). Higher ratios of crystals to vesicles in Etna and Vesuvius lavas increase the Bingham creep viscosity, η_0, and shift it toward smaller strain rates which were unattainable in our torsion experiments. In contrast, the Hawaiian lava sample, with a smaller crystals-to-vesicles ratio, possessed a smaller Bingham creep viscosity which was observable at the lower strain rates of the torsion apparatus (10^{-3} s^{-1}).

If a material has a strain rate-dependent rheology then two different viscosities can be assigned, η_0 and η_∞, which relate to the low and high strain rate limits, respectively. The Cross model then gives the viscosity as:

$$\eta = \eta_\infty + \frac{\eta_0 - \eta_\infty}{1 + (K\dot{\gamma})^m} \quad (6)$$

where m and K are empirical constants and $\dot{\gamma}$ is strain rate (e.g. Barnes, 1999), with m characterising a stretching parameter for shear stress relaxation during the viscoelastic transition. For a Maxwell body rheology, $m = 2$. In the operational window of the oscillatory shear apparatus, only η_0 can be measured. The high strain rate viscosity, η_∞, is interpreted as the effective viscosity of a fluid at high strain rates or stresses. In the case of lavas, it corresponds to the results of field or laboratory experiments in which high strains induced by the measurement disrupt the internal structure of the lava.

The high-temperature data in Fig. 10a have been fitted with Cross curves (assuming that $\eta_0 \gg \eta_\infty$, and using $m = 1$) and the values of η_0

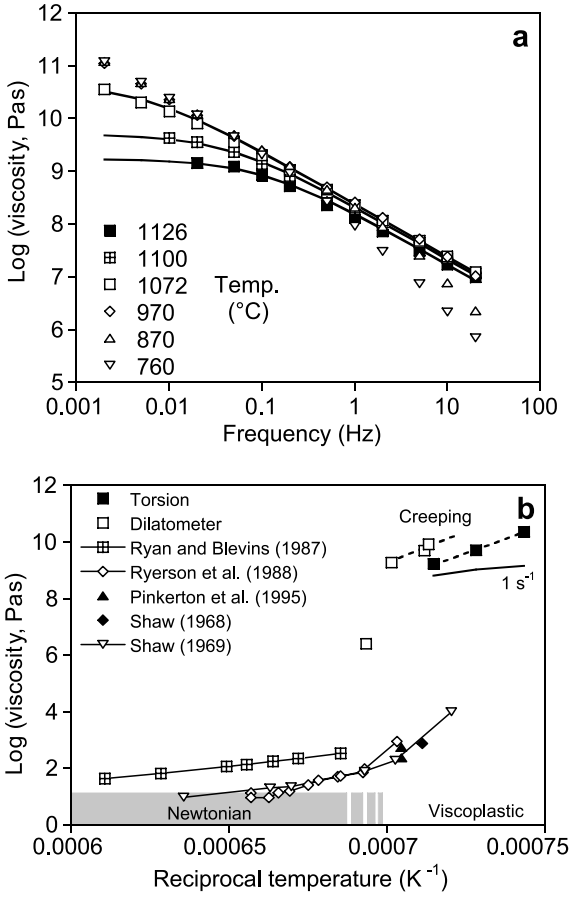

Fig. 10. Dynamic viscosity of the Hawai′i sample. In panel a, the high temperature values of $G''(\omega)/\omega$ are given, demonstrating the decreasing dependence on frequency at low frequencies. The curves show the results of using a Cross model in order to extract the zero-shear viscosity (see text). Fitting parameter of Eq. 5 $m = 1$ at all temperatures, $K = 1.6\log(\eta_0$ Pa s) = 9.23 at 1126°C, 3.7 and 9.7 at 1100°C, 30 and 10.65 at 1072°C. In panel b, the zero-shear viscosity values η_0 obtained for the Hawai′i lava sample are compared with those given by dilatometer (Bagdassarov, 2000) and rotational viscometer (Shaw, 1969; Shaw et al., 1968; Ryan and Blevins, 1987; Ryerson et al., 1988; Pinkerton et al., 1995) experiments on Hawaiian basalt lavas. There is good agreement between the dilatometer and the torsional results, with the slightly greater values from the dilatometer being expected due to the effect of compression viscosity on extracting shear viscosity values from the pure shear experiments (Bagdassarov and Dingwell, 1992). The gradient of the dashed best fit lines represents an activation energy for viscous flow of ~950 kJ mol^{-1}. The plot demonstrates the ~three order of magnitude change in viscosity which occurs around 7.0×10^{-4} K^{-1} (~1155°C) and separates the high-temperature, Newtonian region from the lower-temperature, viscoplastic region. The 1 s^{-1} line indicates the torsion results at unit shear rates which are more applicable for comparison with the rotational viscometer measurements. High values of η_0 obtained in torsion and dilatometer, small strain–stress experiments relate to the creep-type rheology displayed by lava when its internal structure is not destroyed by the measurements. Field experiments carried out at high stresses and strains show η_∞, or a viscoplastic viscosity, expressed when the internal structure (the organisation of vesicles and crystals) of the lava is altered by the viscometer or the flow itself.

obtained are plotted in Fig. 10b along with other viscosity measurements made with a parallel-plate viscometer (a Bähr® high-temperature dilatometer, University Bayreuth (Bagdassarov, 2000)) and rotational viscometers (Shaw, 1969; Shaw et al., 1968; Ryan and Blevins, 1987; Ryerson et al., 1988; Pinkerton et al., 1995). The parallel-plate viscometer uses shear rates of 10^{-5}–10^{-7} s^{-1}, compared with equivalents of $\sim 10^{-2}$–10^{2} s^{-1} for the torsion apparatus. The activation energy for viscous flow obtained by the dilatometer and torsion experiments (given by the gradient of the dashed lines in Fig. 10b) is $\sim 950 \pm 5$ kJ mol^{-1}. The small offset (0.67 log units) between the two lines is due to the effect of the volume (or bulk) viscosity of a porous sample, η_v, which affects the parallel-plate deformation results of the dilatometer experiments. The pure shear deformation used in the dilatometer gives a compressional viscosity, η_c, which is usually related to the shear viscosity by $\eta_c/3$. However, this is valid only for incompressible samples (which have an infinite volume viscosity), and is therefore not applicable to material with $\sim 50\%$ porosity, which will have a finite volume viscosity. For high-porosity materials, the relationship:

$$\eta_c = \eta_v + \tfrac{4}{3}\eta_s \tag{7}$$

is appropriate (e.g. Bagdassarov and Dingwell, 1992). Thus measured values should be corrected for a finite-volume viscosity, the value of which is unknown. From Fig. 10b the compressional viscosity data from the dilatometer experiments are related to the simple shear viscosity results of the torsion experiments, η_s, by $\eta_c \approx 3 \times 10^{0.67} \eta_s$, or $10^{1.15}\eta_s$. Applying Eq. 7 thus gives $\eta_v \approx 12.7\eta_s$ (at $\sim 50\%$ porosity). The theoretical dependence of the volume viscosity as a function of porosity has been considered elsewhere (Prud'homme and Bird, 1978; Aksel, 1995), with the classical formula:

$$\eta_v = \frac{4}{3}\frac{\rho^2}{\rho_0(\rho_0 - \rho)}\eta_s^0 \tag{8}$$

derived for small concentrations of vesicles in a fluid, where ρ_0 is the density of fluid, ρ is the density of the suspension and η_s^0 is the viscosity of the fluid without vesicles. Converting η_s^0 to η_s by $\eta_s^0 \approx 0.2\eta_s$ (for $\sim 50\%$ porosity, Fig. 5, Rust and Manga, 2002), gives the theoretical relation of $\eta_v \approx 3.3\eta_s$. The discrepancy between our result and this theoretical estimation may be easily attributed to experimental errors in viscositiy as well as the non-spherical shape of some vesicles and their non-uniform size distribution in the lava samples.

Alternatives to the Cross model were reviewed by Yue and Brückner (1994), who suggested a strain rate-dependent viscosity model depending on three phenomenological constants. Their model is appropriate for parallel-plate viscometry in which significant strain increases during experiments can produce thermal effects and violations of non-slip boundary conditions. However, in the torsion experiments the maximum torque was 10^{-3} N m, and maximum angle deformation 10^{-5} rad, resulting in a negligible heat production ($< 10^{-7}$ J s^{-1}) even at the highest strain rates used.

Field measurements, corrected to unit strain rate, have reported significantly smaller shear viscosities for Hawaiian basalts. Shaw et al. (1968) measured plastic viscosities of 650–750 Pa s at 1130°C and Pinkerton et al. (1995) measured viscosities of 234–548 Pa s at 1146°C (Fig. 8b). Unit shear rate results from the torsion experiments (as given by the fitted Cross models) are five orders of magnitude greater than these field measurements. For Mount St. Helens dacite, Pinkerton and Stevenson (1992) demonstrated that a combination of factors was responsible for a 10 order of magnitude variation within measured and calculated apparent viscosities at sub-liquidus temperatures. For Hawaiian basalt, although differences in volatile content, crystallinity and vesicularity exist between the experimental and the fieldwork samples, the main difference in the results (Fig. 10b) is due to the magnitude of the strain used, with rotational viscometry producing high strains and torsion and dilatometer experiments producing small strains.

When magmas or lavas are subjected to small strains, the rheology is influenced by the deformation of gas bubbles and by the rotation, interaction and small displacement of crystals suspended in the viscous melt matrix. In this case, the rheol-

ogy is controlled by the 'structure' of the material and is consequently relatively high (see Fig. 10b, torsion and dilatometric experiments). For rotational viscometry (either in the field or in laboratory experiments) the strains are much higher and, with time, the material 'structure' becomes disrupted. The increasingly 'unstructured' nature of the material results in a viscous shear thinning response (Barnes, 1997), producing decreased apparent viscosities.

The small stress and strain rate experiments carried out in torsion and dilatometer equipment demonstrate a second, relatively high-viscosity (creep-type rheology), plateau in the viscosity–strain rate dependence (Barnes, 1999) that cannot be observed with high stress or strain rate measurements. However, at temperatures above ~1145–1150°C the groundmass of lava becomes so fluid that the viscosity decreases a few orders of magnitude (Fig. 10b) and the high-viscosity plateau is no longer present. Fig. 10b demonstrates the difference between the η_0 (creep-type) and η_∞ (viscoplastic) viscosities. In the small strain and small stress torsion equipment, the internal structure of the lava sample is not destroyed, and the measured viscosity is of a creep type. This type of viscosity may be expressed in lava dome growth or relaxation processes. In experiments with rotational viscometers, where strains and stresses are considerable, the internal structure of the lava is destroyed and the apparent viscosity is several magnitudes smaller. This type of viscosity will control lava flows over steep topography. Thus, at the same temperature, lavas may possess two viscosities depending on a stress–strain scale and numerical modelling of lava flows should consider the high viscosity and viscoelasticity of lavas when strain rates are below unity.

5. Conclusions

(1) The oscillatory torsional apparatus allows low-strain investigations of shear modulus and internal friction. Experiments carried out on lavas over a range of temperatures (~500–1150°C) and frequencies (20–0.002 Hz) demonstrate that in general the complex shear modulus of lavas decreases with decreasing frequency and increasing temperature. Internal friction is usually <1.

(2) At temperatures close to their eruption temperature (~1080–1100°C) no purely viscous regime was detected for the Etna and Vesuvius samples and their measured creep-type viscosity remained frequency-dependent over the range 20–0.002 Hz. However, results for the Hawai′i sample indicate a shear rate-independent regime for low shear rates at temperatures between ~1070 and 1130°C, with viscosities $>10^9$ Pa s.

(3) The samples from Etna and Vesuvius exhibited extended anelastic behaviour at temperatures within the 'glass transition' temperature of the groundmass, and that may be attributable to the bad cohesion between crystal grains and the groundmass glass. Annealed lava at ~900–950°C possesses a shear modulus of about 15–20 GPa. Below ~800°C, but still within basalt glass transition temperature range, when the dilatometric effects between groundmass glass and crystals are significant, intensive microcracking may be expected and can decrease the shear modulus to 7–10 GPa. By reheating between 700 and 950°C, the characteristic time constant of the lava hardening process may be on a scale of several to a hundred hours.

Acknowledgements

We thank J. Deubener and one anonymous referee for helpful comments that improved the manuscript.

References

Aksel, N., 1995. A model for the bulk viscosity of a non-Newtonian fluid. Contin. Mech. Thermodyn. 7, 333–339.

Atkinson, B.K., 1984. Subcritical crack growth in geological materials. J. Geophys. Res. 89, 4077–4114.

Atkinson, B.K., Meredith, P.G., 1987. The theory of subcritical crack growth with applications to minerals and rocks. In: Atkinson, B.K. (Ed.), Fracture Mechanics of Rocks. Academic Press, London, pp. 111–166.

Bagdassarov, N.S., 2000. Anelastic and viscoelastic behaviour of partially molten rocks and lavas. In: Bagdassarov, N.,

Laporte, D., Thompson, A. (Eds.), Physics and Chemistry of Partially Molten Rocks. Kluwer, Dordrecht, pp. 29–66.
Bagdassarov, N.S., Dingwell, D.B., 1992. A rheological investigation of vesicular rhyolite. J. Volcanol. Geotherm. Res. 50, 307–322.
Bagdassarov, N.S., Dingwell, D.B., 1993. Frequency dependent rheology of vesicular rhyolite. J. Geophys. Res. 98, 6477–6487.
Bagdassarov, N.S., Dingwell, D.B., Webb, S.L., 1993. Effect of boron, phosphorus and fluorine on shear stress relaxation in haplogranite melts. Eur. J. Mineral. 5, 409–425.
Bagdassarov, N.S., Dingwell, D.B., Webb, S.L., 1994. Viscoelasticity of crystal- and bubble-bearing rhyolite melts. Phys. Earth Planet. Inter. 83, 83–89.
Bagdassarov, N.S., Dorfman, A.M., 1998. Viscoelastic behaviour of partially molten granites. Tectonophysics 290, 27–45.
Barnes, H.A., 1999. The yield stress - a review or 'παντα_ρει' - everything flows? J. Non-Newtonian Fluid Mech. 81, 133–178.
Barnes, H.A., 1997. Thixotropy - a review. J. Non-Newtonian Fluid Mech. 70, 1–33.
Belkin, H.E., Kilburn, C.R.J., De Vivo, B., 1993. Sampling and major element chemistry of the recent (A.D. 1631-1944) Vesuvius activity. J. Volcanol. Geotherm. Res. 58, 273–290.
Berckhemer, H., Kampfmann, W., Aulbach, E., 1982. Anelasticity and elasticity of mantle rocks near partial melting. In: Schreyer, W. (Ed.), High-Pressure Researches in Geoscience. E. Schwaizerbart'sche Verlagsbuchhandlung, Stuttgart, pp. 113–132.
Brady, J.B., 1995. Diffusion data for silicate minerals, glasses, and liquids. In: Ahrens, T.J. (Ed.), Mineral Physics and Crystallography: a Handbook of Physical Constants. AGU, Washington, DC, pp. 269–290.
Burkhard, D.J.M., 2001. Crystallisation and oxidation of Kilauea basalt glass: processes during reheating experiments. J. Petrol. 42, 507–527.
Calvari, S., Pinkerton, H., 2002. Instabilities in the summit region of Mount Etna during the 1999 eruption. Bull. Volcanol. 63, 526–535.
Cooper, R.F., Fanselow, J.B., Poker, D.B., 1996. The mechanism of oxidation of basaltic glass: chemical diffusion of network-modifying cations. Geochim. Cosmochim. Acta 60, 3253–3265.
Day, D.E., Rindone, G.E., 1961. Internal friction of progressively crystallised glasses. J. Am. Ceram. Soc. 44, 161–167.
Dersch, O., Zouine, A., Rauch, F., Ericson, J.E., 1997. Investigation of water diffusion into quartz using ion beam analysis technique. Fresenius J. Anal. Chem. 358, 217–219.
Dingwell, D.B., Hess, K.-U., Romano, C., 1998. Extremely fluid behavior of hydrous peralkaline rhyolites. Earth Planet. Sci. Lett. 158, 31–38.
Garcia, M.O., Rhodes, J.M., Ho, R., Ulrich, G., Wolfe, E., 1992. Petrology of lavas from episodes 2-47 of the Pu′u O′o eruption of Kilauea Volcano, Hawaii: evaluation of magmatic processes. Bull. Volcanol. 55, 1–16.
Gribb, T.T., Cooper, R.F., 1998. Low-frequency shear attenuation in polycrystalline olivine: Grain boundary diffusion and the physical significance of the Andrade model for viscoelastic rheology. J. Geophys. Res. 103, 27267–27279.
Gueguen, Y., Woirgard, J., Darot, M., 1981. Attenuation mechanism and anelasticity in the upper mantle. In: Stacey, F.D., Paterson, M.S., Nicholas, A. (Eds.), Anelasticity in the Earth, Geodynamic Series 4. AGU GSA, Boulder, CO, pp. 86–94.
Jackson, I., 1993. Progress in the experimental study of seismic wave attenuation. Annu. Rev. Earth Planet. Sci. 21, 375–406.
Jackson, I., Paterson, M.S., 1987. Shear modulus and internal friction of calcite rocks at seismic frequencies: pressure, frequency and grain size dependence. Phys. Earth Planet. Inter. 45, 349–367.
Johnson, D.H., Toksöz, M.N., 1980. Thermal cracking and amplitude dependent attenuation. J. Geophys. Res. 85, 937–942.
Kampfmann, W., Berckhemer, H., 1985. High temperature experiments on the elastic and anelastic behaviour of magmatic rocks. Phys. Earth Planet. Inter. 40, 223–247.
Lesher, C.E., Hervig, R.L., Tinker, D., 1996. Self diffusion of network formers (silicon and oxygen) in naturally occurring basaltic liquid. Geochim. Cosmochim. Acta 60, 405–413.
Lu, C., Jackson, I., 1998. Seismic-frequency laboratory measurements of shear mode viscolasticity in crustal rocks II: thermally stressed quartzite and granite. Pure Appl. Geophys. 153, 441–473.
Manghnani, M.H., Rai, C.S., Katahara, K.W., 1981. Ultrasonic velocity and attenuation in basalt melt. In: Stacey, F.D., Paterson, M.S., Nicholas, A. (Eds.), Anelasticity in the Earth, Geodynamic Series 4. AGU GSA, Boulder, CO, pp. 118–122.
Marin, G., 1998. Oscillatory rheometry. In: Collyer, A.A., Clegg, D.W. (Eds.), Rheological Measurements. Chapman and Hall, London, pp. 5–46.
Marsh, B.D., 1981. On the crystallinity, probability of occurrence, and rheology of lava and magma. Contrib. Mineral. Petrol. 78, 85–98.
Norton, G., Pinkerton, H., 1997. Rheological properties of natrocarbonatite lavas from Lengai, Tanzania. Eur. J. Miner. 9, 351–364.
Nowick, A.S., Berry, B.S., 1972. Anelastic Relaxation in Crystalline Solids. Academic Press, London.
O'Connel, R.J., Budiansky, B., 1974. Seismic velocities in dry and saturated cracked solids. J. Geophys. Res. 79, 5412–5426.
Pinkerton, H., Herd, R.A., Kent, R.M., Wilson, L., 1995. Field measurements of the rheological properties of basaltic lavas. Lun. Planet. Sci. 26, 1127–1128.
Pinkerton, H., Norton, G., 1995. Rheological properties of basaltic lavas at sub-liquidus temperatures: laboratory and field measurements on lavas from Mount Ethna. J. Volcanol. Geotherm. Res. 68, 307–323.
Pinkerton, H., Stevenson, R., 1992. Methods of determining the rheological properties of magmas at sub-solidus temperatures. J. Volcanol. Geotherm. Res. 53, 47–66.

Pinkerton, H., Sparks, R.S.J., 1978. Field measurements of the rheology of lava. Nature 276, 383–384.

Prud'homme, R.K., Bird, R.B., 1978. The dilatational properties of suspensions of gas bubbles in incompressible fluids. J. Non-Newtonian Fluid Mech. 3, 261–279.

Richet, P., Lejeune, A.M., Holtz, F., Roux, J., 1996. Water and the viscosity of andesite melts. Chem. Geol. 128, 185–197.

Rocchi, V., Sammonds, P., Kilburn, C.R.J., 2002. Flow and fracture maps for basaltic rock deformation at high temperatures. J. Volcanol. Geotherm. Res. 120, 25–42.

Rust, A.C., Manga, M., 2002. Effect of deformation on the viscosity of dilute suspensions. J. Non-Newtonian Mech. 104, 53–63.

Ryan, M.P., Blevins, J.Y.K., 1987. The viscosity of synthetic and natural silicate melts and glasses at high temperatures and 1 bar (10^5 Pascals) pressure and at higher pressures. U.S. Geol. Surv. Bull. 1764, Denver, CO, 455–456.

Ryan, M.P., Sammis, C.G., 1981. The glass transition in basalt. J. Geophys. Res. 86, 9519–9535.

Ryerson, F.J., Weed, H.C., Piwinskii, A.J., 1988. Rheology of subliquidus magmas. 1. Picritic compositions. J. Geophys. Res. 93, 3421–3436.

Sakuma, S., 1953. Elastic and viscous properties of volcanic rocks at high temperatures. Part 3. Oosima lava. Bull. Earthq. Res. Inst. Tokyo 31, 291–303.

Shaw, H.R., Wright, T.L., Peck, D.L., Okamura, R., 1968. The viscosity of basaltic magma: an analysis of field measurements in Makaopuhi lava lake, Hawai'i. Am. J. Sci. 266, 225–264.

Shaw, H.R., 1969. Rheology of basalt in the melting range. J. Petrol. 10, 510–535.

Sparks, R.S.J., Pinkerton, H., 1978. Effect of degassing on rheology of basaltic lavas. Nature 276, 385–386.

Versteeg, V.A., Kohlstedt, D.L., 1994. Internal friction in lithium aluminosilicate glass-ceramics. J. Am. Ceram. Soc. 77, 1169–1177.

Weiner, A.T., Manghnani, M.H., Raj, R., 1987. Internal friction in tholeiitic basalt. J. Geophys. Res. 92, 11635–11643.

Yue, Y., Brückner, R., 1994. A new description and interpretation of the flow behaviour of glass forming materials. J. Non-Cryst. Solids 180, 66–79.